HHS Public Access

Author manuscript

Mucosal Immunol. Author manuscript; available in PMC 2017 April 25.

Published in final edited form as:

Mucosal Immunol. 2017 May ; 10(3): 743–756. doi:10.1038/mi.2016.83.

Age-related spontaneous lacrimal keratoconjunctivitis is accompanied by dysfunctional T regulatory cells

Terry G. Coursey, **Fang Bian**, **Mahira Zaheer**, **Stephen C. Pflugfelder**, **Eugene A. Volpe**, and **Cintia S. de Paiva**

Ocular Surface Center, Dept. of Ophthalmology, Cullen Eye Institute, Baylor College of Medicine, Houston, TX

Abstract

In both humans and animal models the development of Sjögren syndrome (SS) and non-SS keratoconjunctivitis sicca (KCS) increases with age. Here, we investigated the ocular surface and lacrimal gland phenotype of NOD.B10.H2^b mice at 7–14, 45–50, and 96–100 weeks. Aged mice develop increased corneal permeability, CD4$^+$ T cell infiltration and conjunctival goblet cell loss. Aged mice have lacrimal gland (LG) atrophy with increased lymphocyte infiltration and inflammatory cytokine levels. An increase in the frequency of CD4$^+$Foxp3$^+$ Tregs cells was observed with age in the cervical lymph node (CLN), spleen and LG. These CD4$^+$CD25$^+$ lose suppressive ability, while maintaining expression of Foxp3 and producing IL-17 and IFN-γ. An increase Foxp3$^+$IL-17$^+$ or Foxp3$^+$IFN-γ^+ was observed in the LG and LG-draining CLN. In adoptive transfer experiments, recipients of either purified Tregs or purified T effector cells from aged donors developed lacrimal keratoconjunctivitis, while recipients of young Tregs or young T effector cells failed to develop disease. Overall, these results suggest inflammatory cytokine-producing CD4$^+$Foxp3$^+$ cells participate in the pathogenesis of age-related ocular surface disease.

Keywords

keratoconjunctivitis; Non-obese diabetic mouse; Sjögren's syndrome; T regulatory cells; IL-17; IFN-γ

Introduction

The aging process at the ocular surface is poorly understood. In Sjögren's syndrome (SS) and non-SS keratoconjunctivitis sicca (KCS), as with most other autoimmune diseases, age

Corresponding author: Cintia S. de Paiva, M.D., Ph.D., Ocular Surface Center, Cullen Eye Institute, Baylor College of Medicine, 6565 Fannin Street, NC505G, Houston, TX 77030, cintiadp@bcm.edu, Tel.: +1 713 798 4732; fax: +1 713 798 1457.

Author Contributions

Terry G. Coursey- Designed and performed experiments, analysis, and wrote a majority of the manuscript; Fang Bian- Performed experiments and analysis, and reviewed the manuscript; Mahira Zaheer- Performed experiments and analysis, and reviewed the manuscript; Stephen C. Pflugfelder- Designed experiments and contributed to writing of the manuscript; Eugene A. Volpe- Performed experiments and analysis, and reviewed the manuscript; Cintia S. de Paiva- Designed and performed experiments, analysis, and co-wrote the manuscript.

is a major risk factor. The processes responsible for aging, in general, remains controversial and there is no accepted unifying theory. Several theories have been proposed to explain the aging process. These include “error theories” in which aging occurs in response to DNA damage, posttranslational modification, oxidative or metabolic stress. (1–3) Other theories include “programmed theories” in which genes are switched on or off with age (programmed longevity) or in which the biological clock responds to hormones that control the aging process. (1–3) Another programmed theory is one in which immunological responses become dysregulated with age, leading to susceptibility to infectious disease or increased occurrence of autoimmune disease. (4–6)

Both SS and non-SS KCS have been shown to increase in prevalence with age. (7,8) Aging induces structural changes in the lacrimal gland (LG), including atrophy of acinar cells and fibrosis. Preliminary studies suggest that this fibrosis and gland dysfunction is related to inflammatory disease. (9,10) In humans, there is a progressive increase of lymphocytes in the lacrimal glands beginning at around age 40. (7,8) Findings in animal models (in both rat and mouse) parallel human disease with progressive changes beginning at about 12 months of age. (11,12) An increase in the numbers and inflammatory cytokine production of $CD4^+$ and $CD8^+$ T cells and B cells was reported in the LG of aged C57BL/6 mice by our group. (13)

In addition to increased activity of effector cells, a decrease in immune suppression by $CD4^+CD25^+$ $Foxp3^+$ T regulatory cells (Tregs) has been observed in some autoimmune models with age. In many instances the loss of suppression occurs with unchanged or increased numbers of Tregs. (14,15) It has been well documented that Tregs and T helper (Th) cells, both Th1 and Th17 cells, are major players in many autoimmune diseases, including ocular surface diseases like KCS. (16–19) It is also known that the phenotype of these cells is plastic, and dysregulation is responsible for the pathogenesis of several autoimmune diseases. (20–22) Several groups have report the Tregs become dysfunction with age. (23,24) Others have reported that $CD4^+CD25^+$ $Foxp3^+$ Tregs convert to IL-17-producing effector cells. (20,25) These cells maintain suppressive ability and produce moderate amounts of IL-17 and IFN-γ while maintaining expression of Foxp3. (26) IL-$17^+$$Foxp3^+$ T cells express high levels of Treg markers, Foxp3, CD25, glucocorticoid-induced TNFR (GITR), and cytotoxic T-lymphocyte associated protein 4 (CTLA-4). However, they also express retinoic acid receptor-related orphan receptor γt (ROR γt), IL-17, and increased levels of ICOS, CCR6, and IFN-γ (27)

Various mouse models have been used to model the pathogenesis of SS, such as NZB/W F1, the TGF-β1 KO, MRL/lpr, NFS/sld, the CD25KO and the non-obese diabetic (NOD) mouse. (28–31) The NOD mouse has the greatest similarity to human disease as the development of adenitis is accompanied by decreased secretory function in the lacrimal and salivary glands. http://www.sciencedirect.com.ezproxyhost.library.tmc.edu/science/article/pii/S0896841107001102 - bib10 In this study we employ the NOD.B10-$H2^b$ mice. This a congenic strain in which the MHC of NOD was replaced by the MHC of C57BL/10 mice. These mice fail to develop insulitis and type 1 diabetes, but continue to show a mild SS-like disease. (32)

Here, we describe a spontaneous increase in ocular surface and LG immunopathology with increasing age. Increased inflammation was accompanied by increased numbers of $CD4^+CD25^+Foxp3^+$ T cells compared to young controls. $CD4^+CD25^+Foxp3^+$ T cells in old mice were dysfunctional and expressed an altered IL-17^+IFN-γ^+Foxp3^+ phenotype while maintaining Foxp3 expression. This the first study to describe a subset of $CD4^+CD25^+Foxp3^+$ that spontaneously develop with age, lose suppressive ability, produce significant amounts of inflammatory cytokines, and actively participates in development of lacrimal keratoconjunctivitis sicca.

Materials and Methods

Mice

NOD.B10-$H2^b$ mice were purchased from The Jackson Laboratory (Bar Harbor, ME) for establishment of mouse colonies in our vivarium. Male mice from 7 to 100 weeks old were used. All animal experiments were approved by the Institutional Animal Care and Use Committee at Baylor College of Medicine and adhered to the Association for Research in Vision and Ophthalmology Statement for the Use of Animals in Ophthalmic and Vision Research. At least 32 animals were used per age group: 5 for histology; 6–8 for real-time PCR, 8–10 for flow cytometry, 8–10 for tear collection, and 6–8 for *in vitro* Treg assay. All old mice were visually examined for tumors prior to use.

Measurement of corneal permeability

Corneal epithelial permeability to Oregon Green Dextran (OGD; 70,000 molecular weight; Invitrogen, Eugene, OR) was assessed by instilling 0.5 μL of OGD onto the ocular surface one minute before euthanasia, as previously described.(16) Corneas were rinsed with PBS and photographed under fluorescence excitation at 470 nm. The severity of corneal OGD staining was graded in digital images in the 2 mm central zone of each cornea by 2 masked observers, using the NIS Elements software (Nikon, Melville, NY). Four to six mice (8–12 eyes) per each group were examined in two different sets of experiments.

Tear Washings and EGF Enzyme-Linked Immunosorbent Assay (ELISA)

Tear fluid washings were collected from 12 animals/group/age (7–14 weeks (W), 45–50W, and 96–100W) in two independent experiments using a previously reported method. (33) One sample consisted of tear washings from both eyes of one mouse pooled (2 μL) in PBS + 0.1% bovine serum albumin (8 μL) and stored at −80°C until the assay was performed. Results are presented as means ± SD (pg/mL).

Tear Volume Measurements

Phenol red threads were used to measure tear volume, as previously described. (34) Briefly, a phenol red impregnated thread (Zone-Quick; Showa Yakuhin Kako Co., Tokyo, Japan) was held in the lateral canthus of each eye for 20 seconds. A color change from yellow to red occurs in the thread when tears are absorbed. The distance wet by tears was converted to volume according to a previously published standard. (34)

Histology, PAS Staining, and IHC

Five extraorbital LGs and eyes from each group (7–14 weeks, 45–50 weeks, and 96–100 weeks), were surgically excised, fixed in 10% formalin, embedded in paraffin, and 8-μm sections were cut. Sections were stained with H&E for evaluating morphology and with PAS reagent for measuring goblet cell (GC) density, and images were acquired and processed as previously published. (35)

For immunohistochemistry, five extraorbital LGs and eyes from each group (7–14 weeks, 45–50 weeks, and 96–100 weeks) were embedded in optimal cutting temperature compound (VWR, Suwanee, GA) and flash frozen in liquid nitrogen. Sagittal 8-μm sections were cut with a cryostat (HM 500; Micron, Waldorf, Germany) and placed on glass slides that were stored at −80°C. Immunohistochemistry was performed to detect cells in the conjunctiva and LGs stained positively for CD4 (clone H129.9; 10 μg/mL), CD8 (clone 53–6.2, 10 ug/mL) B220 (clone 30F11, 20 ug/mL) (BD Bioscience, San Diego, CA) and Foxp3 (clone FJK-16S, 20 μg/mL) (eBioscience). $CD4^+$ T cells and GC density was determined by counting cells in three sections (at least 100 μm apart) from six different animals of each strain and at each time point was evaluated. Positively stained cells were counted in the GC-rich area of the conjunctiva, over a length of at least 500 μm in the epithelium and to a depth of 75 μm below the epithelial basement membrane in the stroma, for a distance of at least 500 μm (NIS Elements software).

RNA isolation and Real-time PCR

Total RNA from conjunctiva or the corneal epithelium was extracted using a QIAGEN RNeasy Plus Micro RNA isolation kit (Qiagen) following the manufacturer's protocol. Conjunctiva or extraorbital LG was surgically excised. One sample equaled the tissue pooled from both eyes or both LGs of each animal. After isolation, the concentration of RNA was measured and cDNA was synthesized using the Ready-To-Go™ You-Prime First-Strand kit (GE Healthcare). Real-time PCR was performed using specific Taqman probes for IFN-γ (*Ifng*) (Mm00801778_m1), IL-17A (*Il17a*) (Mm0043918_m1), IL-4 (*Il4*) (Mm00445259M_m1), IL-13 (*Il13*) (Mm99999190_m1), IL-10 (*Il10*) (Mm00439614_m1), TGF-β1 (*Tgfb1*) (Mm00441724), TNF-α (*Tnfa*) (Mm99999068_m1), IL-1β (*Il1b*) (Mm00434228_m1 genes), ROR γT (*Rorc*) (Mm00441139_m1), ICOS (*Icos*) (Mm00497600_m1), CCR6 (*Ccr6*) (Mm01700299_m1), Foxp3 (*Foxp3*) (Mm00475162_m1), GITR (*Tnfrsf1*) (Mm00437136_m1), CTLA-4 (*Ctla4*) (Mm00486849) (Taqman Universal PCR Master Mix AmpErase UNG) in a commercial thermocycling system (StepOnePlus™ Real-Time PCR System, Applied Biosystems), according to the manufacturer's recommendations. The beta-2 microglobulin (β2m) (*B2m*) (Mm00437762_m1) gene was used as an endogenous reference for each reaction. The results of quantitative PCR were analyzed by the comparative C_t method in which the target of change = $2^{-\Delta\Delta^{Ct}}$ and were normalized by the C_t value of β2m and the mean C_t of relative mRNA level in 7–14 week age group. Gene expression of 3–4 mice per strain per time point in two independent experiments with a total of 6–8 mice was determined.

Lacrimal Gland Inflammation Scores and Calculation of Lymphocytes Infiltration

H&E stained lacrimal gland sections were examined by light microscopy (10X). Infiltration scores were assigned according to the following criteria of White and Casarett (36): 0- indicated no foci of mononuclear cells was observed; 1- indicated 1 to 5 foci (more than 20 cells per focus); 2- indicated more than 5 foci were visible but without tissue damage; 3- indicated more than 5 foci with moderate tissue damage; 4 indicated extensive mononuclear infiltration with severe tissue destruction. Scores were assigned by two masked independent observers and averaged. The area of lymphocytic infiltration was circumscribed in digital images of H&E-stained sections. The percentage infiltration was calculated as area of infiltration × 100/total area using NIS Elements Software.

Flow Cytometric Analysis

Right and left extraorbital LGs from one mouse per age group were excised and pooled into a single sample from mice at 7–14W, 45–50W, or 96–100W (n = 12 animals/group divided into three independent experiments with four samples per group/age/experiment). Whole LGs were digested in collagenase type IV (Gibco, 17104-019) (0.1% in Hank's Balanced Saline Solution (HBSS)) for 1 hr at 37C in an orbital shaker. Single-cell suspensions of LGs containing 1×10^6 cells were prepared as previously described after collagenase digestion. (37) Briefly, single-cell suspensions of collagenase-digested LGs were stained with anti-CD16/32, followed by cell surface staining as follows: anti–CD4-fluorescein isothiocyanate (FITC; GK1.5; BD Pharmingen, San Diego, CA), anti–CD8α-phosphatidylethanolamine (PE; clone 53–6.7; BD Pharmingen) or anti-CD8α-PE-Cy7 (BD Pharmingen 552877), anti-B220- allophycocyanin (APC) (clone RA3-6B2; BD Pharmingen), anti-CD161 (NK1.1)-BV650 (Bioledgend 108736), anti-$\gamma\delta$ TCR-BV510 (Bioledgend 118131) and anti-$\alpha\beta$ TCR-AF647 (ThermoFisher HM3621).

For CD4-FITC (BD Bioscience, clone GK1.5), CD25-PE (BD Pharmingen, clone PC61) and Foxp3- APC (eBioscience, San Diego, CA, clone FJK-16-S), single-cell preparations of splenocytes obtained from young mice were stained with the same antibodies and served as positive controls. The gating strategy used in this study was as follows: lymphocytes and monocytes were individually identified on the basis of forward scatter and side scatter properties, subsequently gated on the basis of forward scatter height versus forward scatter area (singlets 1), then gated on side scatter height versus side scatter area (singlets 2). Propidium iodide exclusion was used to discriminate live cells.

For intracellular cytokines staining, single cell suspensions were obtained and 1 x 10^6 cells were incubated for five hours with 1 Ql/ml Golgi Stop (BD Bioscience), 1 Ql/ml Golgi Plug (BD Bioscience), PMA (1Qg/ml) (Sigma, St. Louis, MO), ionomycin (1 Qg/ml) (Sigma) in 1 mL in complete RPMI. Cells were stained with blue fluorescent reactive dye (Life Technologies, Grand Island, NY) for 30 mins. prior to incubation with Foxp3 Fixation/ Permeabilization working solution (eBioscience) for 18 hrs. Cells were washed with 1X Permeabilization solution and incubated with anti-CD16/32, followed by staining with anti-CD4-FITC (BD Bioscience, clone GK1.5), IL-17-PE (eBioscience, clone eBio17B7), anti-Foxp3-APC (eBioscience, FJK-16S), anti-IFN-γ-PacificBlue (Biolegend, San Diego, CA, clone XMG1.2), and anti-CD45-AlexaFluor 700 (Biolegend, clone 30F11). The following

gating strategy was used: dead cells were excluded by gating blue dye versus CD45+ cells, subsequently gated on the basis of forward scatter height versus forward scatter area (singlets 1), then gated on side scatter height versus side scatter area (singlets 2). Cells were then gated on $CD4^+$ cells and $Foxp3^+$ IFN-γ^+ or $Foxp3^+$IL-$17A^+$ cells were evaluated. A BD LSRII Benchtop cytometer was used for flow cytometry, and data were analyzed with BD Diva software version 6.7 (BD Pharmingen) and FlowJo software version 10. (Tree Star Inc., Ashland, OR).

$CD4^+CD25^+$ Regulatory T cell isolation

$CD4^+CD25^+$ Regulatory T cells were isolated via a two-step procedure in which $CD4^+$ T cells were pre-enriched by depletion of unwanted cells. The $CD4^+$ T cell fraction were incubated with anti-CD25-PE antibody and then magnetically labeled with microbeads and positively selected for $CD4^+CD25^+$ T cells. This was performed according to the manufacturers' instructions with a $CD4^+CD25^+$ Regulatory T cell isolation kit (Miltenyi Biotec, Auburn, CA; 130-091-041) on 7-14W or 45-50W NOD.B10.$H2^b$ mice. These cells were used to perform regulatory T cell assays or collection for quantitative gene expression. Purity of $CD4^+CD25^+$ isolation was confirmed by flow cytometry by CD4, CD25, and Foxp3 staining (supplemental figure 2b).

Regulatory T cell assay

$CD4^+CD25^-$ cells (T responders - Tresps) and $CD4^+CD25^+$ cells (Regulatory T cells - Tregs) were isolated and co-cultured at Tresps: Tregs- 1:1 (1×10^5: 1×10^5 cells), 2:1 (1×10^5: 0.5×10^5 cells), 4:1 (1×10^5: 0.25×10^5 cells) ratios or alone in an anti-CD3 antibody coated 96-well plate for 72 hours. The assay was setup with four wells per experimental group. A colorimetric Cell Proliferation WST-1 Reagent (Roche) proliferation assay was performed by adding 10 QL per 100 QL of culture media and incubated for the last four hours of the co-culture period, as previously reported. (38–41) The absorbance was read at 420 nm with a reference wavelength of 600 nm according to the manufacturer's instructions. Inhibition of proliferation was calculated by subtraction of blank (media alone) and divided by the absorbance of Tresps cultured alone. Data is presented as the percentage of total proliferation of Tresps alone. Results presented are the combined results of three independent experiments.

Multiplex cytokine immunobead assay (Luminex)

Serum samples from young or old mice (n=10) or Treg assay supernatants (from three wells for each experimental group) were collected and cytokine production was determined by Luminex assay. Samples were added to wells containing the appropriate cytokine bead mixture that included mouse monoclonal antibodies specific for IL-4 IL-13, IFN-γ, IL-17 (Upstate-Millipore, Billerica, MA). Serial dilutions of the above cytokines were added to wells in the same plate as the mouse samples to generate a standard curve. The plates were incubated overnight at 4°C to capture the cytokines by the antibody-conjugated fluorescent beads. After three washes with assay buffer, 25 QL of biotinylated secondary cytokine antibody mixture was applied for 1.5 h in the dark at room temperature. The reactions were detected with streptavidin–phycoerythrin using a Luminex 100 IS 2.3 system (Austin, TX,

USA). The limit of detection of this assay was 3.4 pg/ml for IFN-γ; 3.4 pg/ml for IL-4; 3.75 pg/ml for IL-13, and 3.19 pg/ml for IL-17.

Adoptive transfer experiments

$CD4^+CD25^+$ or $CD4^+CD25^-$ cells from 7–14 week or 45–50 week old mice were isolated from the spleens and CLN as stated above. $CD4^+CD25^+$ or $CD4^+CD25^-$ cells (2×10^6) were transferred intraperitoneally (i.p.) to 8W old T cell deficient recombination activating protein 1 (RAG1KO) mice. Experiments were performed five weeks after adoptive transfer of $CD4^+CD25^+$ or $CD4^+CD25^-$ cells. Each group contained three to four recipient mice.

Statistical Analysis

Sample size and power calculations were performed using Statmate software based on preliminary studies. Statistical analyses were performed with Graph Pad Prism software (Graph Pad, Inc, version 6). Data was first evaluated for normality with the Kolmogorov-Smirnov normality test. Appropriate parametric (two-way ANOVA or t-test) or non-parametric (Mann-Whitney U or Wilcoxon) statistical tests were used to make comparisons between two groups.

Results

Aged male NOD.B10.H2^b mice have a spontaneous dry eye ocular surface phenotype

Previous studies examining models of SS have focused on LG pathology. Here, we examined the ocular surface disease phenotype of aged NOD.B10.H2^b mice. Hallmarks of dry eye pathology include increased corneal permeability, $CD4^+$ T cell infiltration, conjunctival goblet cell loss and increased expression of inflammatory cytokines (16,42,43). To assess corneal permeability, the fluorescent Oregon green dextran dye (OGD) was instilled in each eye, as previously described. (35) OGD uptake was significantly increased with age (at both 45 and 96 weeks; Figure 1a and c). Confirming dry eye pathology, an age-related increase in $CD4^+$ T cell infiltration was observed in the conjunctiva by immunohistochemistry (Figure 1b and d). In agreement with these findings, a significant decrease in mucin filled conjunctival goblet cells was observed with increasing age as measured by PAS staining (Figure 1e). As expected, an increase in the gene expression of the inflammatory cytokines, IFN-γ and IL-17A, and MHC class II was observed in the conjunctiva with age by qPCR. Conjunctival goblet cell homeostatic promoting factor, IL-13, did not change with age (Figure 1f). These results indicate a progressive increase in ocular surface pathology with advanced age in NOD.B10.H2^b mice.

To determine which population of lymphocytes were producing inflammatory cytokines, flow cytometry experiments were performed in the conjunctiva and the CLN of 7–14W and 45–50W mice. As seen in supplemental figure 1a, $CD4^+$ T cells and $CD8^+$ T cells are predominant lymphocytes, followed by other $CD45^+$ cells (presumably B cells and myeloid cells). NK, NKT, and $\gamma\delta$ T cells make up the other populations in these tissues. Only $CD4^+$, $CD8^+$, and $\gamma\delta$ T cells make IFN-γ and IL-17 in these tissues (supplemental figure 1b).

Aged male NOD.B10.H2^b mice have lacrimal gland pathology

Next, we examined the LG pathology that accompanies age in NOD.B10.H2^b mice. Gross examination of the LGs showed LG atrophy and a progressive loss of cellular components, including acinar cells with aging (Figure 2a). To quantify LG pathology, inflammation scores were assigned to LG sections, according to the parameters stated in the methods sections (Figure 2c) and to account the size of foci we calculated the foci area as a percentage of the total glandular area (Figure 2d). In order to rule out strain specificity of the observed phenotype, LGs were examined from aged C57BL/6 mice, which share the same H2^b haplotype. As seen in figures 2b–d, C57BL/6 mice also develop spontaneous LG pathology with increased age but at a slower rate. These results suggest that C57BL/6 mice develop a disease phenotype similar to NOD.B10.H2^b mice, however, the genetic predisposition of NOD.B10.H2^b mice accelerates disease making this a useful model for aging studies (Figure 2c). Paradoxically, we observed that EGF concentration and tear volume (measured with the phenol red cotton-thread technique) increased with age in NOD.B10.H2^b mice (Figure 2e and f), as previously reported in another aged inbred strain (13). In order to assess the inflammatory state of aged NOD.B10.H2^b mice, we examined the expression of inflammatory cytokines and the infiltration of lymphocytes into the LG. The gene expression of IFN-γ, IL-17A, IL-1β, and TNF-α significantly increased with age in the LG. Interestingly, IL-13 also increased, indicating not only Th1 and Th17-associated cytokines but also Th2-associated cytokines in the LG (Figure 2g). In agreement, increased infiltration of CD4$^+$, CD8$^+$, and B220$^+$ cells was observed in the LG with age by immunohistochemistry and this was quantified by flow cytometry (Figure 2h and i). These observations led to the conclusion that age in NOD.B10.H2^b mice leads to LG pathology similar to the one observed in DED and SS patients.

Systemic inflammation in NOD.B10.H2^b mice

We sought to determine if inflammation in NOD.B10.H2^b mice was exclusive to the eye or LG. To address this, we measured the levels of cytokines in the serum of 7–14W and 96–100W NOD.B10.H2^b mice. A significant increase in the serum levels of IFN-γ and IL-17A, cytokines produced by Th1 and Th17 cells, respectively, was observed (Figure 3c and d). The levels of the Th2-associated cytokines, IL-4 and IL-13, did not change (Figure 3a and b). To further examine this, we determined the frequency of splenic CD4$^+$ T cells that produced IFN-γ or IL-17A in 7-14W and 45-50 W mice. A significant increase in the frequency of CD4$^+$IFN-γ^+ and CD4$^+$IL-17$^+$ was observed in the spleen with age by flow cytometry (Figure 3e and f). This indicates that a Th1 and Th17 systemic immune response occurs with age in NOD.B10.H2^b mice.

Aged NOD.B10.H2^b mice have an increase in CD4$^+$Foxp3$^+$ cells

In spite of increased inflammation, a significant increase of CD4$^+$Foxp3$^+$ was observed in aged NOD.B10.H2^b mice. An increase in the infiltration of Foxp3$^+$ cells was observed in the lacrimal gland as seen by immunohistochemistry with age (Figure 4a). To quantify this, the percentage of CD4$^+$Foxp3$^+$ cells was determined by flow cytometry in LG, submandibular gland (SMG), CLN and spleens of 7–14W and 45–50W NOD.B10.H2^b mice. A significant increase in CD4$^+$Foxp3$^+$ occurs with age in the LG, CLN, and spleen (Figure 4b). We also

examined the effect of age on other glands, such as SMG, in these mice. No changes in clinical inflammation scores or cellular infiltration with age were observed in the SMG (data not shown). Interestingly, $CD4^+Foxp3^+$ have the highest frequency in the aged LG. The LG-draining CLN have increased frequency of $CD4^+Foxp3^+$ cells with age, whereas the spleen has a modest increase in frequency in $CD4^+Foxp3^+$ cells (Figure. 4b). To quantify the expression of Foxp3 the MFI of in $CD4^+Foxp3^+$ was determined. All tissues examine had a significant increase in the expression of Foxp3 (Figure 4c). Paradoxically, the increase of $CD4^+Foxp3^+$ cells occurs despite of increased disease severity, suggesting dysfunction of the suppressive ability of these cells.

Aged mice have an increase in inflammatory cytokine-producing $CD4^+Foxp3^+$ cells

This prompted us to examine the population of $CD4^+Foxp3^+IL\text{-}17^+$ or $CD4^+Foxp3^+IFN\text{-}\gamma^+$ cells in the LG, CLN and spleens of 7–14W and 45–50W mice. As seen in representative plots (Figures 4d and e) and the combined data (Figure 4g) an increase with in $Foxp3^+IL\text{-}17^+$ and $Foxp3^+IFN\text{-}\gamma^+$ was observed in the LG and CLN. Only an increase in the $Foxp3^+IFN\text{-}\gamma^+$ population was observed in the spleen with age. These results suggest that Tregs maintain Foxp3 expression while acquiring the ability to produce IL-17 and IFN-γ. Additionally, these data show an increase in $CD4^+$ IFN-γ^+ (Foxp3 negative) and $CD4^+IL\text{-}17^+$ (Foxp3 negative) cells, suggesting the loss of suppressive ability of Tregs with age (Figures 4d and e). No significant increase was observed in $Foxp3^+IL\text{-}17^+IFN\text{-}\gamma^+$ cells with age in any tissue (Figure 4g). To demonstrate our gating strategy for these experiments, the fluorescence minus one (FMO) (Figure 4f) and no stimulation control plots (supplemental figure 2a) are presented.

We then examined the gene expression of this cell population for inflammatory or suppressive cytokine genes, markers of Tregs, and markers for $CD4^+Foxp3^+IL\text{-}17^+$ cells. To accomplish this, $CD4^+CD25^-$ (T responders; Tresps) and $CD4^+CD25^+$ (Tregs) cells were isolated from the spleens and CLNs of 7–14W (young) or 45–50W (old) NOD.B10.$H2^b$ mice by magnetic bead separation (supplemental figure 2b). A significant increase of IFN-γ, IL-4, and IL-10 was seen in old Tresps compared to young Tresps (Figure 5a). This indicates that old Tresps have greater cytokine production than young Tresps and suggests a general uncontrolled phenotype of these cells. A significant increase for IL-17A and IL-10 was observed in old Tregs in agreement with the increase of $IL\text{-}17^+$ cells seen in figure 5a. A change in the expression of IFN-γ between young and old Tregs was not observed and may be due to a limitation of the isolation as the cells were pooled from both the CLN and spleen to obtain enough cells. TGF-β1 and 2 and TNF-α gene expression did not change (data not shown). It has been reported in the literature that Treg conversion to effector cells is accompanied by increased expression of CCR6, a chemokine receptor expressed by Th17 cells. (44,45) Accordingly, we examined the expression of CCR6 and RORγt, the transcription factor of IL-17 producing cells, and observed an increase in these markers in both old Tresps and Tregs, indicating an increase in IL-17 producing cells. Interestingly, Foxp3 expression increased in Treps and was unchanged in old Tregs. The small increase in Foxp3 expression in Tresps may be due to a contaminating population of $Foxp3^+$ cells that remained after cell isolation. This occurred concurrently with increased production of IL-17A. This is consistent with previous studies demonstrating the phenotype of

IL-17^{+}Foxp3^{+} and the expression of ICOS increased in old Tregs, however, these cells maintain suppressive ability. (27) The expression of cytotoxic T-lymphocyte-associated protein 4 (CTLA-4) decreased in old Tregs, suggesting less suppressive ability. Glucocorticoid-induced TNFR family related gene (GITR) expression did not significantly change with age (data not shown). Overall, these results suggest that with age, mice spontaneously acquire an inflammatory IL-17^{+}Foxp3^{+} or IFN-γ^{+}Foxp3^{+} phenotype.

CD4^{+}CD25^{+} Tregs are dysfunctional in aged NOD.B10.H2^{b} mice

With an increase in CD4^{+}CD25^{+} cells, we sought to determine their suppressive ability in this model. Mixed lymphocyte assays were performed to assess the suppressive ability of Tregs in aged NOD.B10.H2^{b} mice. Again, CD4^{+}CD25^{-} (T responders; Tresps) and CD4^{+}CD25^{+} (Tregs) cells were isolated from 7–14W (young) or 45–50W (old) NOD.B10.H2^{b} mice. To determine the ability of Tresps and Tregs to proliferate, each cell type was incubated for 72 hrs. in anti-CD3 coated plates and WST was added the last four hours of incubation. Only Tresps proliferated in response to anti-CD3 stimulation (Figure 4b). To test suppressive ability, Tresps and Tregs were incubated at a 1:1, 2:1, and 4:1 ratios (Tresps: Tregs) for 72 hrs. in anti-CD3 coated plates. WST was added the last four hours. As seen in figure 5c, young CD4^{+}CD25^{+} Tregs effectively suppressed young Tresps. However, old CD4^{+}CD25^{+} Tregs showed significantly less ability to suppress the proliferation of young Tresps. Likewise, young Tregs are able to suppress young Tresps significantly more than old Tresps, indicating an increase in proliferation of Tresps with aging (Figure 5c).

To examine the ability of Tregs to regulate cytokine production the concentration of IFN-γ and IL-17A was measured in culture supernatant by Luminex assay. Importantly, the same pattern of suppression is observed with IFN-γ, as young Tregs are able to suppress IFN-γ production by young Tresps and old Tresps by 50% and 40%, respectively. By contrast, old Tregs were unable to suppress the production of IFN-γ by either young or old Tresps (Figure 5d). Similarly, old Tregs were unable to suppress the production of IL-17 by either young or old Tresps. Interestingly, co-cultures with old Tregs with young Tresps had an eight-fold increase of IL-17A compared to young Tresps alone and an even greater increase than co-cultures containing young Tregs: young Tresps. Old Tregs: old Tresps co-cultures had a three-fold increase in IL-17A compared to old Tresps alone (Figure 5e).

Aged dysfunctional Tregs are potentially pathogenic

In order to determine if Tregs from 45-50W old mice mediate disease adoptive transfer studies were performed. Tregs (CD4^{+}CD25^{+}) or Tresps (CD4^{+}CD25^{-}) cells were isolated from the spleens and CLNs of 7–14W and 45–50W mice as stated above (see Supplemental Fig 2b for an example). Young (8W old) T cell deficient RAG1KO mice were i.p. injected with 2 x 10^{6} Tregs or Tresps cells. Disease parameters were measured after five weeks. LGs of recipient mice that received aged Tregs or Tresps cells had a significant increase in periductal infiltration of CD4^{+} T cells (Figure 6a). CD4^{+} T cell infiltration was quantified by flow cytometry and indicated a significant increase in CD4^{+} T cells, more specifically CD4^{+}IFN-γ^{+} cells, compared to recipients that received Tregs or Tresps cells from 7–14W mice (Figure 6b). Infiltration into the LG did not change when comparing Tregs and Tresps cells in old mice, demonstrating that old Tregs and Tresps both infiltrate the LG and produce

similar levels of IFN-γ. Examination of GC density in the conjunctiva indicated that young Tregs nor Tresps mediate GC loss in recipient mice. However, Tregs and Tresps from aged mice significantly reduced GC density compared to mice that received young Tregs or Tresps (Figure 6c). Tregs and Tresps from aged mice mediate GC loss at similar levels. To quantify LG pathology, inflammation scores were assigned to LG sections and the size of the foci area as a percentage of the total glandular area was calculated, as in figure 2. Adoptive transfer of old Tregs or Tresps yielded increased LG inflammation scores compared to transfer of young Tregs or Tresps (Figure 6d). Likewise, the percentage of total area with T cell infiltration increase in recipients that received young Tregs or Tresps (Figure 6e). These results indicate that Tregs from aged mice lose suppressive ability and may possibly participate in mediating SS-like disease.

Discussion

Aging is a risk factor for development of DED, SS, and many other autoimmune diseases. Although the pathological changes that occur with age have been described in both humans and animal models, the mechanisms of this process are poorly understood. There is increasing evidence that the ocular surface epithelial disease that develops in DED and SS is the result of inflammation. (16,42) These changes are accompanied by and may be worsened by decreased LG secretion and conjunctival goblet cell density or increased tear evaporation due to lipid tear deficiency. In both humans and animals models, DED and SS are mediated by $CD4^+$ T cells that predominately produce IFN-γ and IL-17A. (16,43,46,47) Although the autoantigen(s) have not been definitively described, the immune response depends on resident ocular surface dendritic cells that are activated in response to dry eye or SS autoantigens and present antigens to lymphocytes in regional draining lymph nodes. (48) The most prevalent risk factors are age and sex (7), so we hypothesized that changes in the immune response would occur with age and these changes would be translated to the ocular surface. To test this hypothesis we examined the immunological changes that occur with age at the ocular surface, lacrimal gland, and regional draining lymph nodes of male NOD.B10-$H2^b$ mice, as male NOD mice develop dacryoadenitis, while females will have sialodenitis (49). However, NOD.B10-$H2^b$ do not develop type I diabetes. (32,50) Our previous published studies (13) and figure 2 show that C57BL/6 mice have the same disease phenotype that naturally occurs with age, however NOD.B10.$H2^b$ develop disease sooner, making this a useful model for aging studies.

Our results indicated that aging induced the phenotype of DED, characterized by increased corneal barrier disruption, decreased density of conjunctival GCs, and an increase in $CD4^+$ T cell infiltration in the conjunctiva. This was also accompanied by increased expression of IFN-γ, IL-17A, and MHC class II transcripts in the conjunctiva. Previous studies have shown that IFN-γ induces goblet cells apoptosis via endoplasmic reticulum stress and cornification of conjunctival epithelial cells. (43,46,47,51–53) IL-17A increases the activity of MMPs that induce corneal permeability. (16,19) This occurred with both the 45–50W and the 96–100W mice. These results were similar to those observed in our previous study that examined aging in the C57BL/6 mouse strain and implies a generalized aging phenotype that is not inbreed-strain specific. (13)

In the LG, we observed gross atrophy of the LG, lymphocytic infiltration and loss of acinar cells that progressed with aging. To examine LG gland function, EGF and tear volume were examined. In spite of LG pathology, old mice had an increase in EGF concentration in tears and also tear volume. Age-induced changes in tear parameters (such as decreased tear volume, tear meniscus height, and tear flow) are often found in the aged population. (54–56) In various animal models, mixed results have been observed with an increase, decrease, or no change in tear volume. (13,57–59) The overall tear volume is the composite of fluid secretion by the LG, ocular surface epithelium, and conjunctival goblet cells. An increase in tear volume can be due to leakage of conjunctival blood vessels during ocular surface inflammation. We did not record body weights of aging mice and it is possible that tear volume would decrease if tear volumes are normalized by body weight. We recently reported that in another SS model, the C57BL/6.NOD-Aec1Aec2 mice have increased tear volume with aging. Moreover, the ratio of IgA (produced by LG) and IgG and IgM (plasma immunoglobulins) in tears did not increase with aging from 4–20 weeks, while an increase of IgA/IgG and IgA/IgM was noted in wild-type mice, indicating reduced IgA secretion in the autoimmune strain.(60) Similarly, increased tear volume was also observed in the Spdef null mouse which lacks conjunctival goblet cells but has an inflammatory cell infiltration. (58)

The expression of inflammatory cytokines, IFN-γ, IL-17A, IL-1β, and TNF-α significantly increased with age within the LG. In agreement with this, an increase in $CD4^+$ T cells and $CD8^+$ T cells and B cells was observed in the LG by IHC and flow cytometry. In humans, lymphocyte infiltration has been detected and increases with age in individuals over 40 years of age.(61) Increased lymphocytes and inflammatory cytokines lead to a chronic fibrotic inflammatory disease of the LG. (11,62)

We next asked if this disease was limited to the LG and ocular surface or was systemic with age. The presence of inflammatory cytokines in serum and an increase $CD4^+$IFN-γ^+ cells and $CD4^+$IL-17^+ cells in the spleen with age indicate a systemic autoimmune response that can be manifested at the ocular surface and LG. With this, we examined the numbers of $CD4^+CD25^+Foxp3^+$ Tregs in the LG, CLN, and spleen. In spite of increased autoimmune disease, there was a significant increase in the frequency of these cells in the LG, CLN and spleen with age. The effect of aging on Tregs is not understood and conflicting results have been reported. (63) It has been reported that Tregs increase the spleen and lymph nodes in mice and this was correlated with decreased protection from pathogens. (64) (65) (66) There are reports that increased infiltration of $Foxp3^+$ cells is positively correlated with increased lymphocyte infiltration and increase disease severity in the lacrimal and salivary gland of SS patients. (67,68) Overall, there is ample evidence to suggest that $CD4^+$ Tregs increase with age, (69) although it not understood why these cells increase with age or what induces the accumulation.

This led us to examine the function of Tregs in aged animals with ocular surface disease. Others have reported that Tregs lose suppressive ability with age influencing autoimmunity. (23,24,63) Our results indicate that $CD4^+CD25^+$ T cells maintain Foxp3 expression but lose suppressive ability with age. There are reports of Tregs becoming “pathogenic exTregs” that lose Foxp3 expression and gain the phenotype of Th17 cells. (20) Other studies suggest that

Tregs can maintain Foxp3 expression while acquiring the ability to produce small amounts of inflammatory cytokines. However, these cells maintain suppressive ability. (15) It is important to note that the change in Treg function in our studies occurred spontaneously with increased age. In addition to losing suppressive ability, $Foxp3^+$ cells in our model acquired the ability to produce significant amounts of IFN-γ and IL-17. Paradoxically, $Foxp3^+$ cells produce similar levels of IFN-γ as $CD4^+CD25^-$ cells. Interestingly, $CD4^+CD25^+$ Tregs have significantly increased production of IL-17 compared to $CD4^+CD25^-$ cells. This suggests that these cells acquire a greater ability to produce inflammatory cytokines in LG and LG-draining CLN with age and this occurs to a greater extent that it does in the spleen.

Our adoptive transfer studies suggest that aged Tregs, in addition to loss of suppressive ability, mediate disease through production of inflammatory cytokines, while maintaining Foxp3 expression. These results suggest that old Tregs may become pathogenic themselves. However, it is not possible to obtain an extremely pure cell population of Tregs to perform adoptive transfer experiments. Thus, we undoubtedly transferred some $CD4^+$Foxp3 negative cells (Tresps) in the Treg fraction. It is possible that old Tregs do not suppress overactive Tresps present in the cell fraction which expand and mediate disease. Due to this, it is inherently difficult to conclude that old Tregs are themselves pathogenic and can independently mediate disease. It is also possible that conversion of Tregs to Tresps occurs due to the influence of the lymphopenic environment. However, this only occurs in the old Treg group, as with transfer of young Tregs there was very little infiltration or glandular inflammation, suggesting that dysfunction of Tregs occurs with age. Overall, our results suggest that dysregulation and acquisition of an effector cell phenotype of Tregs could to be a major mechanism for increased incidence of DED and SS with age. Whether the change in phenotype is a consequence of inflammation or the cause of inflammation is still unknown.

There are several other reports of $Foxp3^+IL\text{-}17^+$ or $Foxp3^+IFN\text{-}\gamma^+$ cells. (45,70,71) However, in these models, $Foxp3^+$ cells maintain suppressive ability. To the best of our knowledge this the first report of a population of Tregs that express Foxp3 and are potentially pathogenic in nature. Thus, this may be an undiscovered $Foxp3^+$ cell population that occurs in mucosal tissues with age. Our results suggest that this mechanism may contribute to the pathogenesis observed in patients with SS. The major strength of this work is the spontaneous nature (with age) in which Tregs, while maintaining Foxp3 expression, produce IL-17 and IFN-γ and may contribute to pathology.

Supplementary Material

Refer to Web version on PubMed Central for supplementary material.

Acknowledgments

We would like to thank Kevin Tesareski for technical assistance performing experiments in this manuscript. We would also like to thank Dr. Achim Krauss for providing some of the 100W NOD.B10.$H2^b$ mice.

This work was supported by Fight for Sight Grants-in-aid (CSDP), EY018888 (CSDP), NIH T32 (A1053831) (FB), EY11915 (SCP), NIH Core Grants-EY002520 & EY020799, Research to Prevent Blindness, the Oshman Foundation, William Stamps Farish Fund, the Hamill Foundation and by the Cytometry and Cell Sorting Core at

Baylor College of Medicine which is funded by the NIH National Institute of Allergy and Infectious Diseases grants P30AI036211, NCI P30CA125123, and NCRR S10RR024574.

Abbreviations

Treg	T regulatory cell
ANOVA	analysis of variance
DED	dry eye disease
GC	goblet cells
LG	lacrimal gland
CLN	cervical lymph nodes
OCT	optimal cutting temperature compound
OGD	Oregon Green dextran
PBS	phosphate-buffered saline
RT-PCR	real-time polymerase chain reaction
Th	real-time polymerase chain reaction T helper
SS	Sjögren Syndrome
NOD	non-obese diabetic

Reference List

1. Rocha EM, Alves M, Rios JD, Dartt DA. The Aging Lacrimal Gland: Changes in Structure and Function. Ocul Surf. 2008; 6:162–174. [PubMed: 18827949]
2. Sergiev PV, Dontsova OA, Berezkin GV. Theories of aging: an ever-evolving field. Acta Naturae. 2015; 7:9–18. [PubMed: 25926998]
3. Cohen AA. Complex systems dynamics in aging: new evidence, continuing questions. Biogerontology. 2015
4. Fulop T, Witkowski JM, Pawelec G, Alan C, Larbi A. On the immunological theory of aging. Interdiscip Top Gerontol. 2014; 39:163–176. [PubMed: 24862019]
5. Castelo-Branco C, Soveral I. The immune system and aging: a review. Gynecol Endocrinol. 2014; 30:16–22. [PubMed: 24219599]
6. DeVeale B, Brummel T, Seroude L. Immunity and aging: the enemy within? Aging Cell. 2004; 3:195–208. [PubMed: 15268753]
7. Schaumberg DA, Sullivan DA, Buring JE, Dana MR. Prevalence of dry eye syndrome among US women. Am J Ophthalmol. 2003; 136:318–326. [PubMed: 12888056]
8. Schaumberg DA, Dana R, Buring JE, Sullivan DA. Prevalence of dry eye disease among US men: estimates from the Physicians' Health Studies. Arch Ophthalmol. 2009; 127:763–768. [PubMed: 19506195]
9. Damato BE, Allan D, Murray SB, Lee WR. Senile atrophy of the human lacrimal gland: the contribution of chronic inflammatory disease. Br J Ophthalmol. 1984; 68:674–680. [PubMed: 6331845]
10. BENSON WR. Accerleration of Aging Changes in the Exorbital Lacrimal Gland of the Female Rat. Am J Pathol. 1964; 45:587–597. [PubMed: 14217674]

11. Draper CE, Adeghate E, Lawrence PA, Pallot DJ, Garner A, Singh J. Age-related changes in morphology and secretory responses of male rat lacrimal gland. J Auton Nerv Syst. 1998; 69:173–183. [PubMed: 9696274]
12. Williams RM, Singh J, Sharkey KA. Innervation and mast cells of the rat lacrimal gland: the effects of age. Adv Exp Med Biol. 1994; 350:67–74. [PubMed: 7913287]
13. McClellan AJ, Volpe EA, Zhang X, Darlington GJ, Li DQ, Pflugfelder SC, de Paiva CS. Ocular Surface Disease and Dacryoadenitis in Aging C57BL/6 Mice. Am J Pathol. 2014
14. Thomas DC, Mellanby RJ, Phillips JM, Cooke A. An early age-related increase in the frequency of CD4+ Foxp3+ cells in BDC2.5NOD mice. Immunology. 2007; 121:565–576. [PubMed: 17437531]
15. Zhao L, Sun L, Wang H, Ma H, Liu G, Zhao Y. Changes of CD4+CD25+Foxp3+ regulatory T cells in aged Balb/c mice. J Leukoc Biol. 2007; 81:1386–1394. [PubMed: 17369496]
16. de Paiva CS, Chotikavanich S, Pangelinan SB, Pitcher JI, Fang B, Zheng X, Ma P, Farley WJ, Siemasko KS, Niederkorn JY, Stern ME, Li D-Q, Pflugfelder SC. IL-17 disrupts corneal barrier following desiccating stress. Mucosal Immunology. 2009 May; 2(3):243–53. Epub 2009 Feb 25. [PubMed: 19242409]
17. Chauhan SK, El AJ, Ecoiffier T, Goyal S, Zhang Q, Saban DR, Dana R. Autoimmunity in dry eye is due to resistance of Th17 to Treg suppression. J Immunol. 2009; 182:1247–1252. [PubMed: 19155469]
18. Zheng X, de Paiva CS, Li DQ, Farley WJ, Pflugfelder SC. Desiccating stress promotion of Th17 differentiation by ocular surface tissues through a dendritic cell-mediated pathway. Invest Ophthalmol Vis Sci. 2010; 51:3083–3091. [PubMed: 20130281]
19. Zhang X, Volpe EA, Gandhi NB, Schaumburg CS, Siemasko KF, Pangelinan SB, Kelly SD, Hayday AC, Li DQ, Stern ME, Niederkorn JY, Pflugfelder SC, de Paiva CS. NK cells promote Th-17 mediated corneal barrier disruption in dry eye. PLoS One. 2012; 7:e36822. [PubMed: 22590618]
20. Guo J, Zhou X. Regulatory T cells turn pathogenic. Cell Mol Immunol. 2015
21. Grant CR, Liberal R, Mieli-Vergani G, Vergani D, Longhi MS. Regulatory T-cells in autoimmune diseases: challenges, controversies and--yet--unanswered questions. Autoimmun Rev. 2015; 14:105–116. [PubMed: 25449680]
22. Li X, Zheng Y. Regulatory T cell identity: formation and maintenance. Trends Immunol. 2015; 36:344–353. [PubMed: 25981968]
23. Nishioka T, Shimizu J, Iida R, Yamazaki S, Sakaguchi S. CD4+CD25+Foxp3+ T cells and CD4+CD25-Foxp3+ T cells in aged mice. J Immunol. 2006; 176:6586–6593. [PubMed: 16709816]
24. Schmitt V, Rink L, Uciechowski P. The Th17/Treg balance is disturbed during aging. Exp Gerontol. 2013; 48:1379–1386. [PubMed: 24055797]
25. Komatsu N, Okamoto K, Sawa S, Nakashima T, Oh-hora M, Kodama T, Tanaka S, Bluestone JA, Takayanagi H. Pathogenic conversion of Foxp3+ T cells into TH17 cells in autoimmune arthritis. Nat Med. 2014; 20:62–68. [PubMed: 24362934]
26. Kryczek I, Wu K, Zhao E, Wei S, Vatan L, Szeliga W, Huang E, Greenson J, Chang A, Rolinski J, Radwan P, Fang J, Wang G, Zou W. IL-17+ regulatory T cells in the microenvironments of chronic inflammation and cancer. J Immunol. 2011; 186:4388–4395. [PubMed: 21357259]
27. Du R, Zhao H, Yan F, Li H. IL-17+Foxp3+ T cells: an intermediate differentiation stage between Th17 cells and regulatory T cells. J Leukoc Biol. 2014; 96:39–48. [PubMed: 24744433]
28. Nguyen CQ, Peck AB. Unraveling the pathophysiology of Sjogren syndrome-associated dry eye disease. Ocul Surf. 2009; 7:11–27. [PubMed: 19214349]
29. Cha S, Peck AB, Humphreys-Beher MG. Progress in understanding autoimmune exocrinopathy using the non-obese diabetic mouse: an update. Crit Rev Oral Biol Med. 2002; 13:5–16. [PubMed: 12097234]
30. Jabs DA, Prendergast RA, Campbell AL, Lee B, Akpek EK, Gerard HC, Hudson AP, Whittum-Hudson JA. Autoimmune Th2-mediated dacryoadenitis in MRL/MpJ mice becomes Th1-mediated in IL-4 deficient MRL/MpJ mice. Invest Ophthalmol Vis Sci. 2007; 48:5624–5629. [PubMed: 18055812]

31. Rahimy E, Pitcher JD III, Pangelinan SB, Chen W, Farley WJ, Niederkorn JY, Stern ME, Li DQ, Pflugfelder SC, de Paiva CS. Spontaneous autoimmune dacryoadenitis in aged CD25KO mice. Am J Pathol. 2010; 177:744–753. Epub 2010 Jun 21. [PubMed: 20566743]
32. Yoon KC, de Paiva CS, Qi H, Chen Z, Farley WJ, Li DQ, Stern ME, Pflugfelder SC. Desiccating environmental stress exacerbates autoimmune lacrimal keratoconjunctivitis in non-obese diabetic mice. J Autoimmun. 2008; 30:212–221. [PubMed: 17988834]
33. Pitcher J III, de Paiva CS, Pelegrino F, McClellan A, Raince J, Pangelinan S, Rahimy E, Farley W, Stern M, Li D, Pflugfelder S. Pharmacological cholinergic blockade stimulates inflammatory cytokine production and lymphocytic infiltration in the mouse lacrimal gland. Invest Ophthalmol Vis Sci. 2011; 52:3221–3227. [PubMed: 21273534]
34. Stewart P, Chen Z, Farley W, Olmos L, Pflugfelder SC. Effect of experimental dry eye on tear sodium concentration in the mouse. Eye Contact Lens. 2005; 31:175–178. [PubMed: 16021005]
35. Coursey TG, Gandhi NB, Volpe EA, Pflugfelder SC, de Paiva CS. Chemokine receptors CCR6 and CXCR3 are necessary for CD4(+) T cell mediated ocular surface disease in experimental dry eye disease. PLoS One. 2013; 8:e78508. [PubMed: 24223818]
36. White SC, Casarett GW. Induction of experimental autoallergic sialadenitis. J Immunol. 1974; 112:178–185. [PubMed: 4544191]
37. McClellan AJ, Volpe EA, Gandhi NB, Zhang X, Darlington G, De-Quan L, Pflugfelder SC, de Paiva CS. Ocular surface disease and dacryoadenitis in aging C57BL/6 mice. Am J Pathol. 2014
38. Lau KM, Cheng SH, Lo KW, Lee SA, Woo JK, van Hasselt CA, Lee SP, Rickinson AB, Ng MH. Increase in circulating Foxp3+CD4+CD25(high) regulatory T cells in nasopharyngeal carcinoma patients. Br J Cancer. 2007; 96:617–622. [PubMed: 17262084]
39. Dannull J, Schneider T, Lee WT, de RN, Tyler DS, Pruitt SK. Leukotriene C4 induces migration of human monocyte-derived dendritic cells without loss of immunostimulatory function. Blood. 2012; 119:3113–3122. [PubMed: 22323449]
40. Gulden E, Ihira M, Ohashi A, Reinbeck AL, Freudenberg MA, Kolb H, Burkart V. Toll-like receptor 4 deficiency accelerates the development of insulin-deficient diabetes in non-obese diabetic mice. PLoS One. 2013; 8:e75385. [PubMed: 24086519]
41. Qing K, Weifeng W, Fan Y, Yuluan Y, Yu P, Yanlan H. Distinct different expression of Th17 and Th9 cells in coxsackie virus B3-induced mice viral myocarditis. Virol J. 2011; 8:267. [PubMed: 21635745]
42. Niederkorn JY, Stern ME, Pflugfelder SC, de Paiva CS, Corrales RM, Gao J, Siemasko K. Desiccating Stress Induces T Cell-Mediated Sjogren's Syndrome-Like Lacrimal Keratoconjunctivitis. J Immunol. 2006; 176:3950–3957. [PubMed: 16547229]
43. de Paiva CS, Villarreal AL, Corrales RM, Rahman HT, Chang VY, Farley JW, Stern ME, Niederkorn JY, LD-Q, Pflugfelder SC. IFN-$\gamma\gamma$Promotes Goblet Cell Loss in Response to Desiccating Ocular Stress. Invest Ophthalmol Vis Sci 2006. 2006; 47 E-Abstract 5579.
44. Ayyoub M, Deknuydt F, Raimbaud I, Dousset C, Leveque L, Bioley G, Valmori D. Human memory FOXP3+ Tregs secrete IL-17 ex vivo and constitutively express the T(H)17 lineage-specific transcription factor RORgamma t. Proc Natl Acad Sci U S A. 2009; 106:8635–8640. [PubMed: 19439651]
45. Voo KS, Wang YH, Santori FR, Boggiano C, Wang YH, Arima K, Bover L, Hanabuchi S, Khalili J, Marinova E, Zheng B, Littman DR, Liu YJ. Identification of IL-17-producing FOXP3+ regulatory T cells in humans. Proc Natl Acad Sci U S A. 2009; 106:4793–4798. [PubMed: 19273860]
46. Zhang X, Chen W, de Paiva CS, Corrales RM, Volpe EA, McClellan AJ, Farley WJ, Li DQ, Pflugfelder SC. Interferon-{gamma} Exacerbates Dry Eye Induced Apoptosis in Conjunctiva via Dual Apoptotic Pathways. Invest Ophthalmol Vis Sci. 2011
47. de Paiva CS, Villarreal AL, Corrales RM, Rahman HT, Chang VY, Farley WJ, Stern ME, Niederkorn JY, Li DQ, Pflugfelder SC. Dry Eye-Induced Conjunctival Epithelial Squamous Metaplasia Is Modulated by Interferon-{gamma}. Invest Ophthalmol Vis Sci. 2007; 48:2553–2560. [PubMed: 17525184]
48. Schaumburg CS, Siemasko KF, de Paiva CS, Wheeler LA, Niederkorn JY, Pflugfelder SC, Stern ME. Ocular surface APCs are necessary for autoreactive T cell-mediated experimental

autoimmune lacrimal keratoconjunctivitis. J Immunol. 2011; 187:3653–3662. [PubMed: 21880984]

49. Toda I, Sullivan BD, Rocha EM, da Silveira LA, Wickham LA, Sullivan DA. Impact of gender on exocrine gland inflammation in mouse models of Sjogren's syndrome. Exp Eye Res. 1999; 69:355–366. [PubMed: 10504269]
50. Robinson CP, Yamachika S, Bounous DI, Brayer J, Jonsson R, Holmdahl R, Peck AB, Humphreys-Beher MG. A novel NOD-derived murine model of primary Sjogren's syndrome. Arthritis Rheum. 1998; 41:150–156. [PubMed: 9433880]
51. Zhang X, Chen W, de Paiva CS, Volpe EA, Gandhi NB, Farley WJ, Li DQ, Niederkorn JY, Stern ME, Pflugfelder SC. Desiccating Stress Induces CD4(+) T-Cell-Mediated Sjogren's Syndrome-Like Corneal Epithelial Apoptosis via Activation of the Extrinsic Apoptotic Pathway by Interferon-gamma. Am J Pathol. 2011; 179:1807–1814. [PubMed: 21843497]
52. Zhang X, de Paiva CS, Su Z, Volpe EA, Li DQ, Pflugfelder SC. Topical interferon-gamma neutralization prevents conjunctival goblet cell loss in experimental murine dry eye. Exp Eye Res. 2014; 118:117–124. [PubMed: 24315969]
53. Coursey TG, Tukler HJ, Barbosa FL, de Paiva CS, Pflugfelder SC. Interferon-gamma-Induced Unfolded Protein Response in Conjunctival Goblet Cells as a Cause of Mucin Deficiency in Sjogren Syndrome. Am J Pathol. 2016; 186:1547–1558. [PubMed: 27085137]
54. Furukawa RE, Polse KA. Changes in tear flow accompanying aging. Am J Optom Physiol Opt. 1978; 55:69–74. [PubMed: 677249]
55. Patel S, Wallace I. Tear meniscus height, lower punctum lacrimale, and the tear lipid layer in normal aging. Optom Vis Sci. 2006; 83:731–739. [PubMed: 17041318]
56. Mathers WD, Lane JA, Zimmerman MB. Tear film changes associated with normal aging. Cornea. 1996; 15:229–334. [PubMed: 8713923]
57. Kojima T, Wakamatsu TH, Dogru M, Ogawa Y, Igarashi A, Ibrahim OM, Inaba T, Shimizu T, Noda S, Obata H, Nakamura S, Wakamatsu A, Shirasawa T, Shimazaki J, Negishi K, Tsubota K. Age-related dysfunction of the lacrimal gland and oxidative stress: evidence from the Cu,Zn-superoxide dismutase-1 (Sod1) knockout mice. Am J Pathol. 2012; 180:1879–1896. [PubMed: 22440255]
58. Marko CK, Menon BB, Chen G, Whitsett JA, Clevers H, Gipson IK. Spdef null mice lack conjunctival goblet cells and provide a model of dry eye. Am J Pathol. 2013; 183:35–48. [PubMed: 23665202]
59. Modulo CM, Machado Filho EB, Malki LT, Dias AC, de Souza JC, Oliveira HC, Jorge IC, Santos Gomes IB, Meyrelles SS, Rocha EM. The role of dyslipidemia on ocular surface, lacrimal and meibomian gland structure and function. Curr Eye Res. 2012; 37:300–308. [PubMed: 22440161]
60. You IC, Bian F, Volpe EA, de Paiva CS, Pflugfelder SC. Age-related conjunctival disease in the C57BL/6.NOD-Aec1Aec2 Mouse Model of Sjogren Syndrome develops independent of lacrimal dysfunction. Invest Ophthalmol Vis Sci. 2015
61. Nasu M, Matsubara O, Yamamoto H. Post-mortem prevalence of lymphocytic infiltration of the lacrymal gland: a comparative study in autoimmune and non-autoimmune diseases. J Pathol. 1984; 143:11–15. [PubMed: 6737113]
62. Draper CE, Adeghate EA, Singh J, Pallot DJ. Evidence to suggest morphological and physiological alterations of lacrimal gland acini with ageing. Exp Eye Res. 1999; 68:265–276. [PubMed: 10079134]
63. Jagger A, Shimojima Y, Goronzy JJ, Weyand CM. Regulatory T cells and the immune aging process: a mini-review. Gerontology. 2014; 60:130–137. [PubMed: 24296590]
64. Chiu BC V, Stolberg R, Zhang H, Chensue SW. Increased Foxp3(+) Treg cell activity reduces dendritic cell co-stimulatory molecule expression in aged mice. Mech Ageing Dev. 2007; 128:618–627. [PubMed: 17961632]
65. Sharma S, Dominguez AL, Lustgarten J. High accumulation of T regulatory cells prevents the activation of immune responses in aged animals. J Immunol. 2006; 177:8348–8355. [PubMed: 17142731]
66. Lages CS, Suffia I, Velilla PA, Huang B, Warshaw G, Hildeman DA, Belkaid Y, Chougnet C. Functional regulatory T cells accumulate in aged hosts and promote chronic infectious disease reactivation. J Immunol. 2008; 181:1835–1848. [PubMed: 18641321]

67. Christodoulou MI, Kapsogeorgou EK, Moutsopoulos NM, Moutsopoulos HM. Foxp3+ T-regulatory cells in Sjogren's syndrome: correlation with the grade of the autoimmune lesion and certain adverse prognostic factors. Am J Pathol. 2008; 173:1389–1396. [PubMed: 18818377]

68. Sarigul M, Yazisiz V, Bassorgun CI, Ulker M, Avci AB, Erbasan F, Gelen T, Gorczynski RM, Terzioglu E. The numbers of Foxp3 + Treg cells are positively correlated with higher grade of infiltration at the salivary glands in primary Sjogren's syndrome. Lupus. 2010; 19:138–145. [PubMed: 19952070]

69. Raynor J, Lages CS, Shehata H, Hildeman DA, Chougnet CA. Homeostasis and function of regulatory T cells in aging. Curr Opin Immunol. 2012; 24:482–487. [PubMed: 22560294]

70. Feng T, Cao AT, Weaver CT, Elson CO, Cong Y. Interleukin-12 converts Foxp3+ regulatory T cells to interferon-gamma-producing Foxp3+ T cells that inhibit colitis. Gastroenterology. 2011; 140:2031–2043. [PubMed: 21419767]

71. Koenecke C, Lee CW, Thamm K, Fohse L, Schafferus M, Mittrucker HW, Floess S, Huehn J, Ganser A, Forster R, Prinz I. IFN-gamma production by allogeneic Foxp3+ regulatory T cells is essential for preventing experimental graft-versus-host disease. J Immunol. 2012; 189:2890–2896. [PubMed: 22869903]

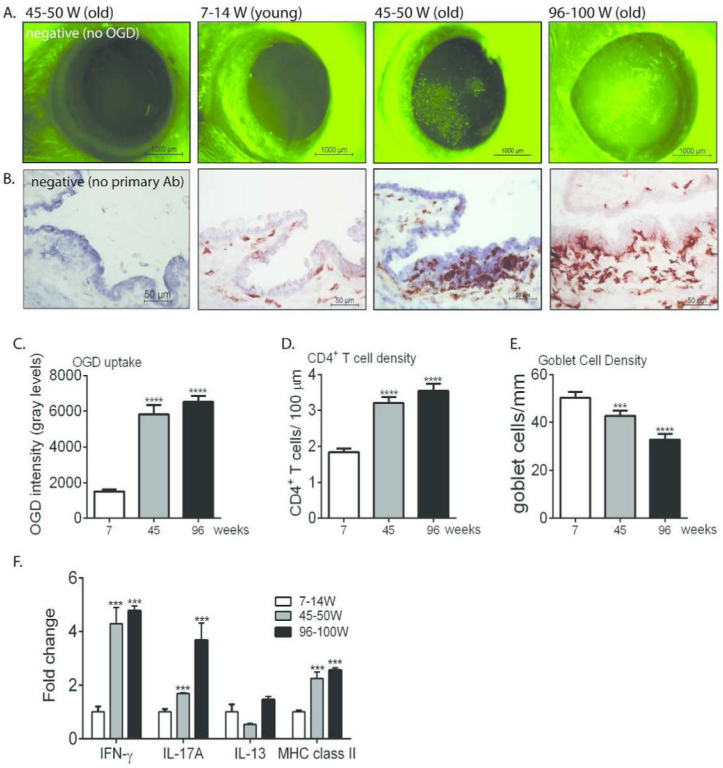

Figure 1. Aged male NOD.B10.H2^{b} mice have a spontaneous dry eye phenotype

A: Representative pictures of the corneas stained with Oregon-Green dextran of 7–14W, 45–50W and 96–100W mice. **B**: Representative images of conjunctiva frozen sections immunostained for CD4 (in red/brown) used to generate the bar graph in D. **C**: Corneal Oregon-Green dextran (OGD) fluorescence intensity score. Bar graphs show means ± SD of three independent experiments with five animals per experiment (10 eyes per experiment, yielding a final sample of 30 eyes per group). **D**: CD4^{+} T cells infiltrating the conjunctival epithelium. Bar graphs show means ± SD of two independent experiments with two to three animals per age, yielding a final sample of five left eyes for each group). **E:** Number of PAS^{+} conjunctival goblet cells counted in paraffin-embedded sections expressed as number per millimeter. Bar graphs show means ± SD of two independent experiments with two to three animals per group, yielding a final sample of five right eyes for each group). **F**: Relative fold expression changes of IFN-γ, IL-17A, IL-13 and MHC class II mRNA in the conjunctiva. Bar graphs show means ± SD of six samples per age (the experiment was repeated twice with similar results). Parametric t tests statistical tests were used to make comparisons between age groups. *$P < 0.05$, **$P < 0.01$, ***$P < 0.001$, ****$P < 0.001$ for comparison between age groups. W - weeks

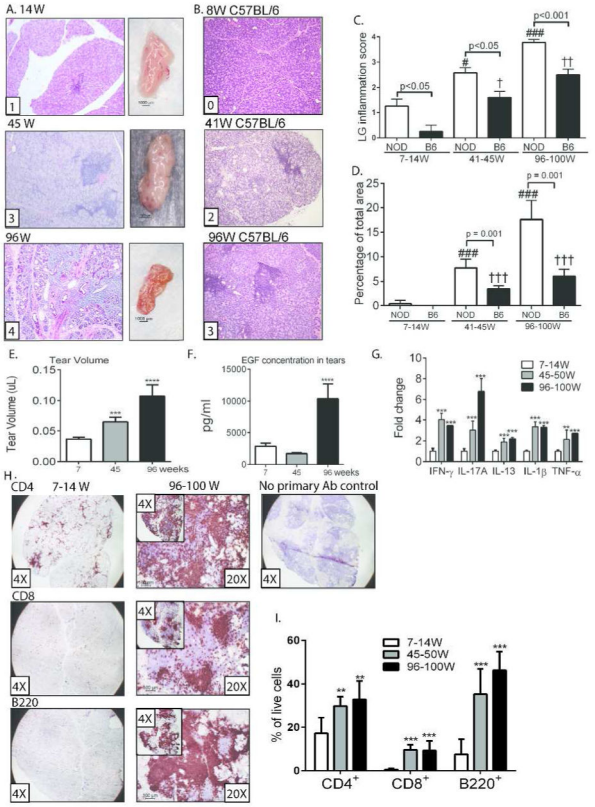

Figure 2. Aged male NOD.B10.H2^b mice have dacryoadenitis

A: Representative pictures of the LGs of 7–14W, 45–50W and 96–100W of H & E stained sections of LG (left) with picture of total LG (right). Inflammation scores of the representative images appear in the lower left inset. **B.** Representative images of the LGs of 8W, 41W and 96W of H & E stained sections of LG of C57BL/6 mice. Inflammation scores of the representative images appear in the lower left inset. **C**: Inflammation scores of LG pathology of NOD.B10.H2^b mice. #$P < 0.05$, ###$P < 0.001$ for comparison between NOD.B10.H2^b age groups. †$P < 0.05$, ††$P < 0.01$ for comparison between C57BL/6 age groups. Two-way Anova followed by Holm-Sidak's comparison test was used to make comparisons of inflammation scores. **D**: Calculation of the foci area as a percentage of the total lacrimal gland area. #$P < 0.05$, ###$P < 0.001$ for comparison between NOD.B10.H2^b age groups. †$P < 0.05$, ††$P < 0.01$ for comparison between C57BL/6 age groups. Two-way Anova followed by Holm-Sidak's comparison test was used to make comparisons of inflammation scores. The data in C and D is the mean of at least five (range five to nine) LGs from different animals. **E.** Tear volumes were measured by phenol red threads tests. Bar graphs show the means ± SD of six to eight animals per group. **F.** Tear EGF concentrations from NOD.B10.H2^b mice were measured by enzyme linked immunosorbent assay. Tear washings from both right and left eyes from one mouse per group were collected and pooled into a single tube, yielding a final sample of 12 individual samples per group divided into three independent experiments with four samples per experiment. **G**: Relative fold expression changes of IFN-γ, IL-17A, IL-13, IL-1β, and TNF-α mRNA in the LG. Bar graphs show means ± SEM of six samples per age (the experiment was repeated twice with

similar results). **H:** Representative images of frozen lacrimal gland sections immunostained for CD4 (upper), CD8 (middle), and B220 (bottom) of 7-14W mice compared to 96–100W mice. As a negative control, 96–100 W LG section was stained without primary antibody (upper right). Insets are 4X and larger images are 20X in the 96–100W group. **I**: Flow cytometric analysis of LG in 7–14W, 45–50W and 96–100W. Right and left extraorbital LGs from one mouse per group were excised and pooled into a single tube, yielding a final sample of 12 individual LG samples per group and age divided into three independent experiments with four samples per experiment. Bar graphs show means ± SD Parametric t tests statistical tests were used to make comparisons between age groups. *$P < 0.05$, **$P < 0.01$, ***$P < 0.001$, ****$P < 0.001$ for comparison between age groups.

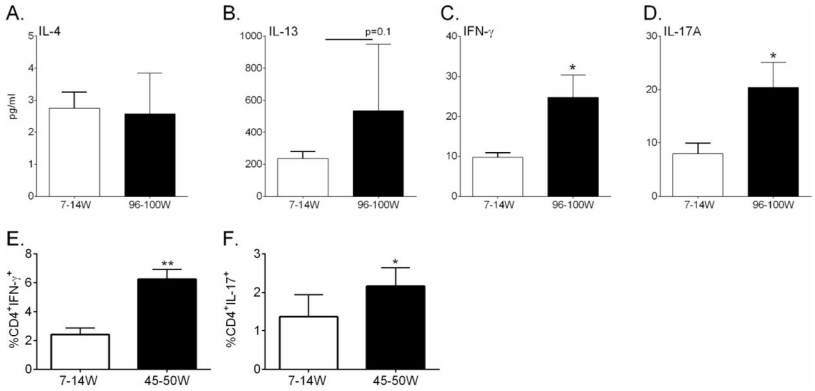

Figure 3. Increase production of cytokines in the serum and lymphoid tissue of aged mice

A–D: The concentration of IL-4 (**A**), IL-13 (**B**), IFN-γ (**C**), and IL-17A (**D**) were measured in the blood serum of 7–14W and 96–100W mice by Luminex assay. Serum was collected from five mice per group. **E–F**: The percentage of $CD4^+IFN\text{-}\gamma^+$ cells (**E**) and $CD4^+IL\text{-}17^+$ cells (**F**) in the spleens of 7–14W and 45–50W mice was determined by flow cytometry. Bar graphs show means ± SD of six to eight animals. Parametric t tests statistical tests were used to make comparisons between age groups. $*P < 0.05$, $**P < 0.01$ for comparison between age groups.

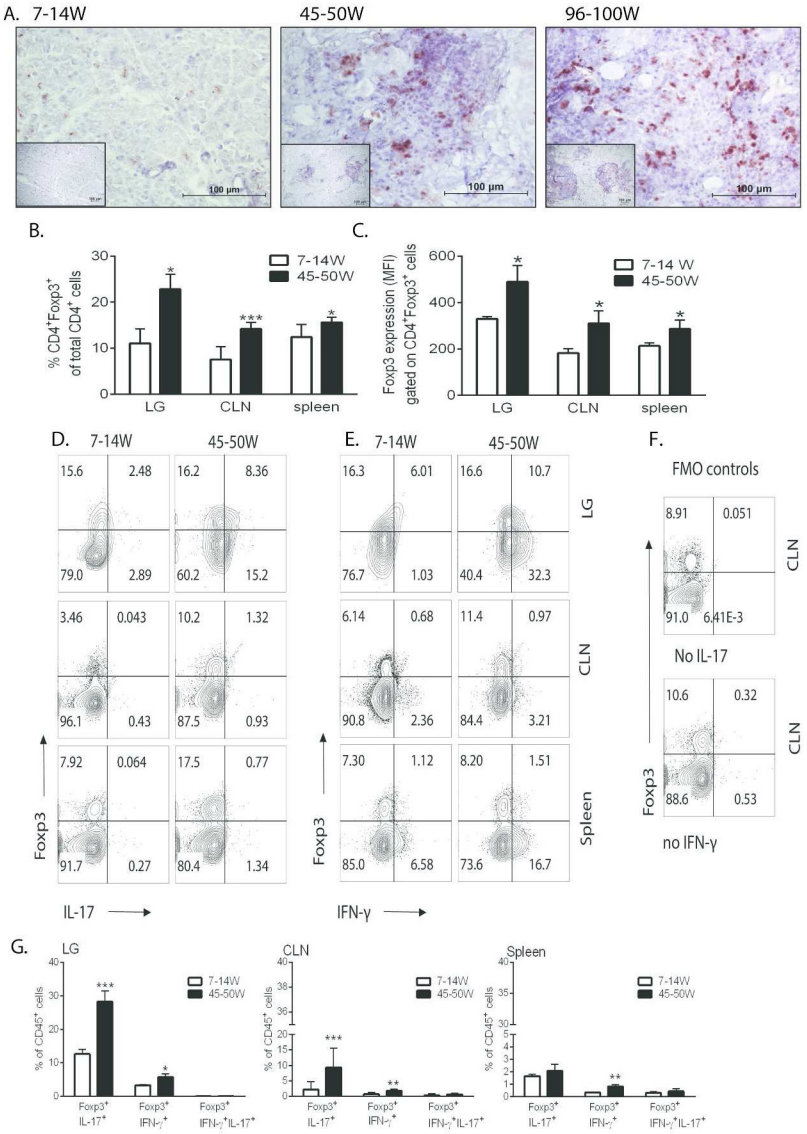

Figure 4. Aged NOD.B10.H2^{b} mice have an increase in CD4^{+}Foxp3^{+} Tregs that produce IL-17 and IFN-γ

A: Immunohistochemical staining for Foxp3 in the LG demonstrated an increase in Foxp3 with increasing age. Magnification is 20X; inset is 4X. **B**: Flow cytometric analysis showing the percentage of CD4^{+}Foxp3^{+} in LG, SMG, CLN, and spleen of 7–14W and 45–50W mice. Lymphocytes were individually identified on the basis of forward scatter and side scatter properties, subsequently gated on the basis of forward scatter height versus forward scatter area (singlets 1), then gated on side scatter height versus side scatter area (singlets 2). Propidium iodide exclusion was used to discriminate live cells; CD4^{+} T cells were gated based on FSC-A properties **C**: Mean fluorescence intensity (MFI) of Foxp3 (MFI) in the LG, CLN and spleen of 7–14W and 45–50W mice. **D–E**: Flow cytometric analysis of LG, SMG, CLN, and spleen indicated an increase Foxp3^{+}IL-17A^{+} cells (D) or Foxp3^{+}IFN-γ^{+} cells (E) in 45–50W mice. Representative plots are shown for each age group. **F**: FMO controls are shown the right. **G**: Bar graphs show cumulative data presented in D and E.

Graphs (B–E, G) show the means ± SD of four- six samples per age (the experiment was repeated three times with similar results).

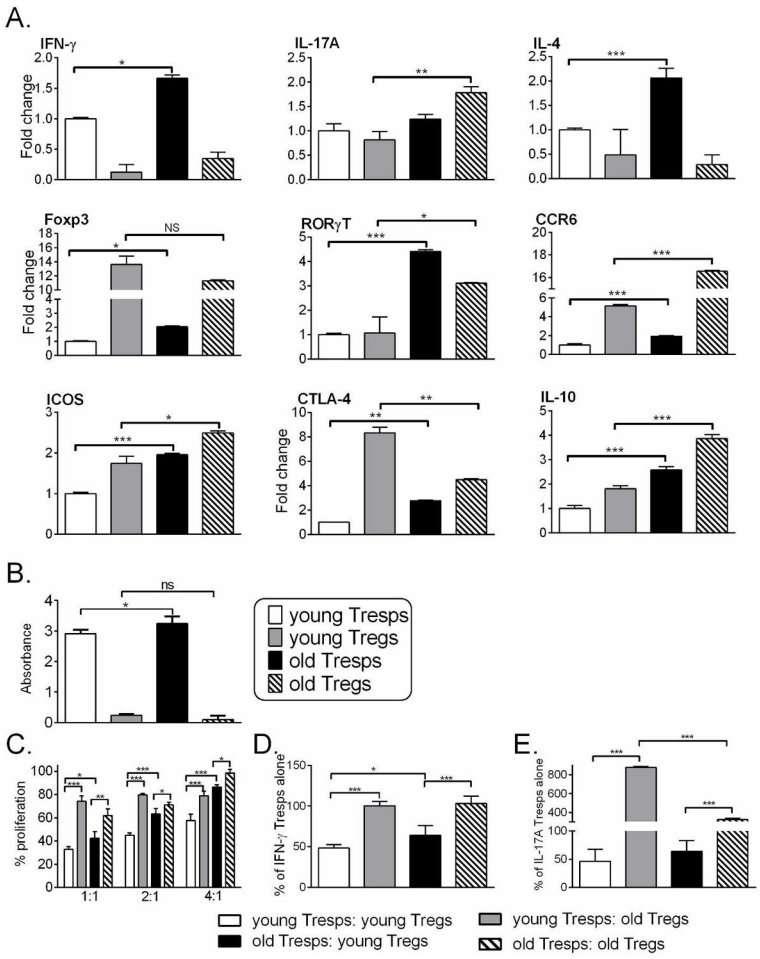

Figure 5. Aged mice develop CD4$^+$CD25$^+$Foxp3$^+$IL-17$^+$ or CD4$^+$Foxp3$^+$IFN-γ^+ cells that have an effector cell phenotype and are dysfunctional

A: Relative fold expression changes in Teffector and Treg marker mRNA of young Tresps (CD4$^+$CD25$^-$), young Tregs (CD4$^+$CD25$^+$), old Tresps and old Tregs. Fold change was determined by comparison to young Tresp cells. Bar graphs show means ± SD of four to six samples per group. **B**: Cell proliferation was measured for young CD4$^+$CD25$^-$ Tresps, young CD4$^+$CD25$^+$ Tregs, old CD4$^+$CD25$^-$ Tresps, and old CD4$^+$CD25$^+$ Tregs with colorimetric Cell Proliferation WST-1 Reagent. **C**: Cell proliferation was measured in co-cultures of Tregs and effector T cell responders (CD4$^+$CD25$^-$; Tresps) from young (7–14W) and old (45–50W) mice. Tregs and Tresps were cultured at a 1:1, 2:1, or 4:1 ratio (Tresps: Tregs) for 72 hrs. % proliferation was determined the by calculating proliferation compared to Tresps without Tregs. Bar graphs show means ± SD of the average of three independent experiments. **D**: The production of IFN-γ was determined by Luminex assay. Co-culture supernatants were collected in triplicate and the percentage of IFN-γ compared to Tresps alone was determined. Bar graphs show a representative experiment of three independent experiments with the same trend. **E:** The production of IL-17A was determined by Luminex assay. Co-culture supernatants were collected in triplicate and the percentage of IL-17A compared to Tresps alone was determined. Bar graphs show a representative experiment of

three independent experiments with the same trend. Parametric t tests statistical tests were used to make comparisons between age groups. *$P < 0.05$, **$P < 0.01$, ***$P < 0.001$, ****$P < 0.001$ for comparison between age groups.

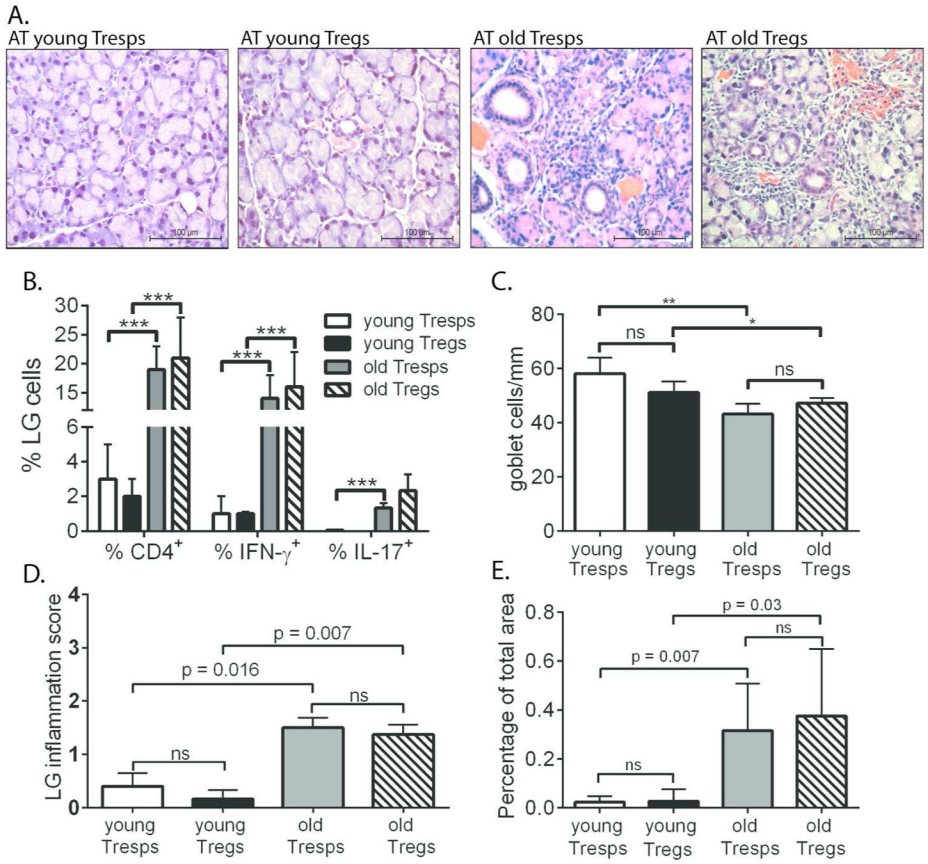

Figure 6. Adoptive transfer (AT) of aged Tregs mediates disease in recipient animals

A: H & E staining of LGs of AT recipients indicated $CD4^+$ T cell infiltration in recipients receiving old Tresps or Tregs. Representative images (40X) are shown for each AT group. **B:** Flow cytometric analysis of recipient LGs indicated an increase $CD4^+$ T cells, specifically $CD4^+IFN\text{-}\gamma^+$ and $CD4^+IL\text{-}17^+$ cells, in mice receiving Tresps or Tregs from 45–50W mice. Bar graphs show means ± SD of four-six samples per AT group. **C.** Number of PAS^+ conjunctival goblet cells counted in paraffin-embedded sections expressed as number per millimeter. Bar graphs show means ± SD of four to six animals per AT group. Parametric t tests statistical tests were used to make comparisons between age groups. $*P < 0.05$, $**P < 0.01$, $***P < 0.001$, $****P < 0.001$. **D:** Inflammation scores of LG pathology of AT recipients. Non-parametric Mann-Whitney U statistical tests were used to make comparisons of inflammation scores. **E:** Calculation of the foci area as a percentage of the total lacrimal gland area. Non-parametric Mann-Whitney U statistical tests were used to make comparisons of inflammation scores. The data in C and D is the mean of four to six LGs from different animals.